Available online at www.sciencedirect.com

ScienceDirect

Procedia Structural Integrity 24 (2019) 233–239

Structural Integrity Procedia

www.elsevier.com/locate/procedia

AIAS 2019 International Conference on Stress Analysis

Monitoring of Li-ion cells with distributed fibre optic sensors

Elena Vergori[a], Yifei Yu[b,*]

[a]Politecnico di Torino – Dipartimento di Ingegneria Meccanica e Aerospaziale (DIMEAS), Corso Duca degli Abruzzi, 24, 10129 Torino, Italy
[b]University of Warwick – Warwick Manufacturing Group (WMG), Coventry CV4 7AL, United Kingdom

Abstract

The in-operando monitoring of surface temperature and strain distribution in 5 Ah Li-ion A5 pouch cells is presented in this work. The measurement is performed through Rayleigh scattering based Distributed Fibre Optic Sensors (DFOS) during cycling at three different C-rates and three different ambient temperature. The sensors were bonded on the pouch cell surface, covering four regions along the shorter cell direction, and on both sides, for a total of eight regions per cell. The distributed temperature and strain gradients were recorded over time. This study aims to contribute to the definition of an effective procedure to real-time monitor temperature and strain gradients in a Li-ion pouch cell during cycling to early detect abnormal conditions that can be critical for the battery state of health and safety. The study also intends to demonstrate the feasibility of the use of these kind of sensors for this application, to be further used for internal in-situ and in-operando monitoring.

Keywords: Li-ion pouch cell; distributed fibre optic sensors; temperature monitoring; strain monitoring.

1. Introduction

In the global mobility scenario, new legislations in various countries all over the world are getting stricter and encourage users to buy electrified vehicles, in order to reduce the use of conventional fossil fuels, to reduce the environmental impact. Li-ion batteries, that represent the main novelty element in battery packs of electrified vehicles, are a very hot topic both in the research and in the industrial field. Many studies, such as Vertiz et al. (2014) and Seong

* Corresponding author. Tel.: +44-776-676-5875; fax: +44-247-657-4907.
E-mail address: yy8186@gmail.com

10.1016/j.prostr.2020.02.020

et al. (2013), are trying to provide answers to open questions on cells degradation in order to develop and tune models that can effectively represent the actual behavior of these cells, on the way to increase cells capacity and cycle life, on how to further reduce the cells cost by using new materials or different process parameters, and finally on how to develop recycling process suitable to dispose of battery packs in a cheap and efficient way.

Li-ion cells are characterized by a safety operating window that consists in voltage, current and temperature limits. Among these quantities, temperature results to be the harder to be controlled, as during operation cells are subjected to temperature gradients due to internal heat generation and heat dissipation, and to thermal conduction among cells in battery modules and packs, as underlined by Raijmakers et al. (2019), Jaiswal (2017).

Furthermore, Liao et al. (2019) and Chen et al. (2005) show that Li-ion performance strongly depend on temperature and thermal gradients in a cell and between cells represent one of the main reasons for uneven cells ageing and shorten life of Li-ion cells. According to Mukhopadhyay and Sheldon (2014), during cycling Li-ion cells also undergo dimensional variations due to the Lithium ions lithiation/delithiation and this influences the cells performance as such stresses can produce fractures and loss in contact between current collectors and the active electrode materials and ultimately lead to capacity fade and eventual failure of a Li-ion cell.

In parallel, thanks to the development of sensors and computational power that allows to process a larger amount of data, studies are also carried out in order to improve the monitoring of battery packs, in order to improve diagnostic algorithms to be implemented on-board the Battery Management System (BMS) of electrified vehicles to predict more accurately which is the actual state of a cell, in terms of both state of charge and state of health, and thus to provide to the final user more accurate information to reduce range anxiety and increase safety, as presented by Smith and Wang (2006), Turrentine (2011). Kim et al. (2019) underlines that currently the BMS monitoring Li-ion cells relies on voltage, current and temperature.

In this work, distributed fibre optic sensors have been used to acquire distributed temperature and strain on a Li-ion pouch cell surface in various operating conditions. These measurements can be used to detect real-time abnormal conditions that can affect the cell and battery pack performance and safety.

Nomenclature

c-OFDR	coherent Optical Frequency Domain Reflectometry
DFOS	distributed fibre optic sensor
FBG	fibre Bragg grating
RTD	resistance temperature detector
TLS	tunable laser source

1.1. Li-ion cells monitoring

In the literature, works published on Li-ion cells temperature and strain monitoring can be distinguished according to two main categories: the number of measurement points, that can either be point monitoring or distributed monitoring, and the sensors location, that can either be external or internal. The most common point sensors used include RTDs, thermocouples and FBGs for temperature monitoring and strain gauges and FBGs for strain monitoring, such as in the works of Waldmann et al. (2016), Goutam et al. (2015) and Lee et al. (2013). All these sensors have been used for both external and internal point sensing. FBGs have also been used as semi-distributed sensors, as their manufacturing process allows to inscribe a certain number of fibre Bragg gratings into the same fibre, but their location must be defined during the design stage. However, as single-point sensors only monitor pre-defined locations, both the number of measurement points and their position definition can become a critical task, especially if the aim of the study is to capture event whose location is not previously known such as a temperature hotspot or a crack formation. In fact, in such cases a wrong sensor positioning can lead to useless measurements.

Some of the major advantages of fibre optic sensors include electrical insulation, electromagnetic immunity, ability to survive to high temperature and in harsh environment, very small dimensions, intrinsically multiplexed. All these characteristics make them suitable for the application of Li-ion cells and eligible also for internal integration, as shown in Nascimento et al. (2019), Ganguli et al. (2017) and Raghavan et al. (2017).

In the present work, it has been studied a possible way to monitor Li-ion cells during operation in order to provide additional information on their actual state and thus improve the accuracy of the estimation of index such as state of charge and state of health, but also to improve safety.

The cells used in this work are A5 pouch cells with surface dimensions of 130 mm and 185 mm respectively in the width and the length directions. Other key cell information include a nominal capacity of 5 Ah, a chemistry characterized by NMC cathode and graphite anode, a maximum charging voltage of 4.2 V and a cut-off voltage of 2.5 V. The monitoring of distributed temperature and strain has been performed using temperature and strain DFOS.

2. Distributed fibre optic sensors and data acquisition system

The sensors used in this work are High-Definition Single-Mode Fibre (SMF) optic. These sensors are available in lengths of up to 20 m and are ideal for making measurements in static and pseudo-static test environments. The sensor structure consists in an inner core with a typical diameter of 8 - 9 μm, a cladding with a diameter of 125 μm, and a coating with a diameter of 155 μm.

The data acquisition system consists in the DFOS interrogator. It works according to the coherent optical frequency domain reflectometry. The coherent Optical Frequency Domain Reflectometry (c-OFDR) is a technique designed to measure back reflections from optical fibre networks and components. It consists in the use of a tunable laser source to generate a swept wavelength interferometry beam of light. This light is used to scan a fibre optic. When the fibre optic is scanned, because of the Rayleigh scattering phenomenon, continually distributed scatter happens throughout the fibre. The backscatter waves generated along the fibre length create and interference pattern. This pattern, called backscattered spectrum, is measured by the detector. The SWI allows to measure the Rayleigh backscatter as a function of position in the fibre optic. As explained by Bao and Chen (2012), the fibre is intrinsically sensitive to temperature and strain as a change in these quantities will produce a measurable change in the way light is backscattered in each fibre location. In known conditions, a fingerprint spectrum is acquired, that is stable and unique. The cross-correlation of the backscattered spectrum and the fingerprint spectra is computed to determine the spectral shift of the scattered light. This frequency shift $\Delta\nu$ can be converted into temperature and strain change by using proper calibration constants, according to Equation 1.

$$\frac{\Delta \nu}{\nu} = K_T * T + K_\varepsilon * \varepsilon \tag{1}$$

The distributed measurement spatial resolution depends on the frequency range swept by a tunable laser ΔF, according to Equation 2.

$$\Delta z = \frac{c}{2n\Delta F} \tag{2}$$

where n is the refractive index of the fibre and ΔF is the frequency swept of the laser, thus the larger is the frequency swept of the laser, the smaller is the spatial resolution. The spatial resolution Δz affects the signal to noise ratio of the measurement. The longer Δz, the better the measurement accuracy. But if temperature or strain vary rapidly in position, a smaller Δz is necessary to prevent distortion in the cross-correlation spectra. The number of measurement points N per laser scan depends on the spatial resolution Δz and thus on the laser scan frequency and on the fibre length L according to Equation 3.

$$N = \frac{L}{\Delta z} \tag{3}$$

Because the sensor is sensitive to both temperature and strain, it is necessary to properly decouple the two contributions of frequency shift before the conversion into physical quantities. To remove the effect of strain it is possible to simply put the sensor in a PolyTetraFluoroEthylene (PTFE) tube that allows the sensor not to be constrained on the surface and thus not to be influenced by strain.

The interrogator has got one measurement channel only, thus, in order to acquire the signal from multiple sensors, a fibre optic switch is used.

3. Setup and experimental test

In the current setup, two cells have been monitored with the same 5 m temperature sensor and 5 m strain sensor. Theoretically, one sensor long enough can be used to monitor all cells, but this would make the manufacturing process and the testing setup more complicated because these sensors are very sensitive and fragile, and it might become difficult to deal with them. Thus, even if these sensors can monitor a very large number of points, a trade-off must always be considered when defining the configuration layout. Additionally, one sensor can be used to monitor both temperature and strain as the PTFE tube can be applied only in a certain region, if the sensor is not under tension. The sensors have been bonded to the pouch cells external surface using epoxy glue. Before the actual gluing process, a small tension has been applied to the strain sensing region. Thus, after the glue was dry, a residual strain was evident in all the bonded regions. In order to be able to measure easily measure strain deriving from actual operating conditions, a former acquisition called tare is acquired and it is subtracted to all the following acquisitions.

The cells have been cycled with three different C-rates, respectively 1C, 3C and 5C, and at three different ambient temperatures, respectively 10 °C, 25 °C and 40 °C. The 1C, 3C and 5C current value, for a 5 Ah cell correspond respectively to 5 A, 15 A and 25 A. According to the fibre optic bend radius limits and the cell free surface, the sensors have been bonded on four regions per side and on both sides, for a total of eight regions per cell, in the cell width direction, for a total of 16 regions per sensor.

The experimental setup consists of a climatic chamber, used to control ambient temperature, a cycler, used to charge and discharge cells according to predefined profiles, an optical interrogator with an optical multiplexer to acquire the optical sensors signal, four pouch cells, a PC with LabVIEW to control the optical equipment and finally the pouch cells with the fibre optic sensors. A setup summary scheme is shown in Fig. 1.

Additionally, 8 thermocouples have been added on each cell surface, two per sensing region, to compare electrical sensors results with optical sensors results. This comparison also allowed to underline the difference in complexity of the setup when using thermocouples that are point sensors, with DFOS.

The test has been performed twice, using two different laser scan frequencies. A first test has been conducted with a scan frequency of 50.0 Hz, which implies a spatial resolution of 5.2 mm and a gage pitch of 2.6 mm. In this test, only temperature has been acquired as this scan frequency guarantees a larger spatial resolution and thus a lower signal to noise ratio. A second test has been conducted with a scan frequency of 23.8 Hz, which implies a spatial resolution of 1.3 mm and a gage pitch of 0.65 mm. In this test both temperature and strain have been acquired as this scan frequency is more suitable when there are high discontinuity along the sensor length because it allows to indulge to these discontinuities and provide a better output. The high discontinuity on the strain sensor are mainly due to the step variation between the sensor region bonded on the pouch cell and the free sensor region. The 16 sensing regions per sensor correspond to about 800 sample points at 50.0 Hz and 3200 sample points at 23.8 Hz.

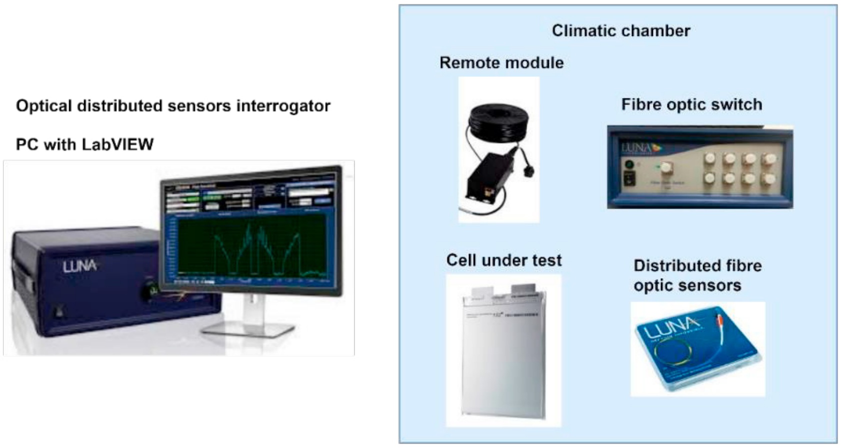

Fig. 1. Experimental setup.

4. Results and observations

This section will be divided into two paragraphs. A first one where temperature results from the 50 Hz test will be presented and a second one where the strain and temperature results from the 23.8 Hz test will be presented.

4.1. Temperature gradients

The considered testing conditions represent an ideal condition as each cell is separate from all other cells, thus it can dissipate heat to surrounding environment that is always cooler as there are no heat sources. Nevertheless, already in this condition it is possible to identify surface temperature gradients. Other test outcome include that during cycling the cell temperature is higher in the surface central region and on the positive terminal. Also, when cycling at 3C and 5C the temperature profile over time is monotonous, while when cycling ad 1C temperature increases, then decreases and finally increases according to a monotonous trend. Furthermore, a much higher temperature gradient is registered during higher C-rate cycling, due to the higher heat generation.

In Fig. 2, the temperature results of the two thermocouples point sensors have been overlapped to the fibre optic sensors distributed results. In the present test, two thermocouples have been used in each region. The figure shows the temperature evolution over time and the point sensors limitation becomes very clear. The thermocouples setup implies the necessity to have the physical space to locate the thermocouples on the cell surface, the necessity of data acquisition channels and finally the wires deriving from these connections. On the contrary, the DFOS allow to implement a much simpler setup, with less acquisition ports and much more sample point with a small spatial resolution.

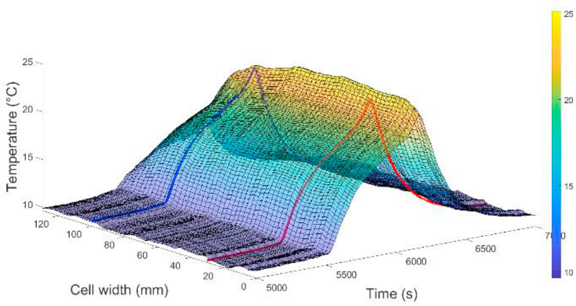

Fig. 2. Comparison between the output of point sensors thermocouples and distributed fibre optic sensors. Comparison over time evolution.

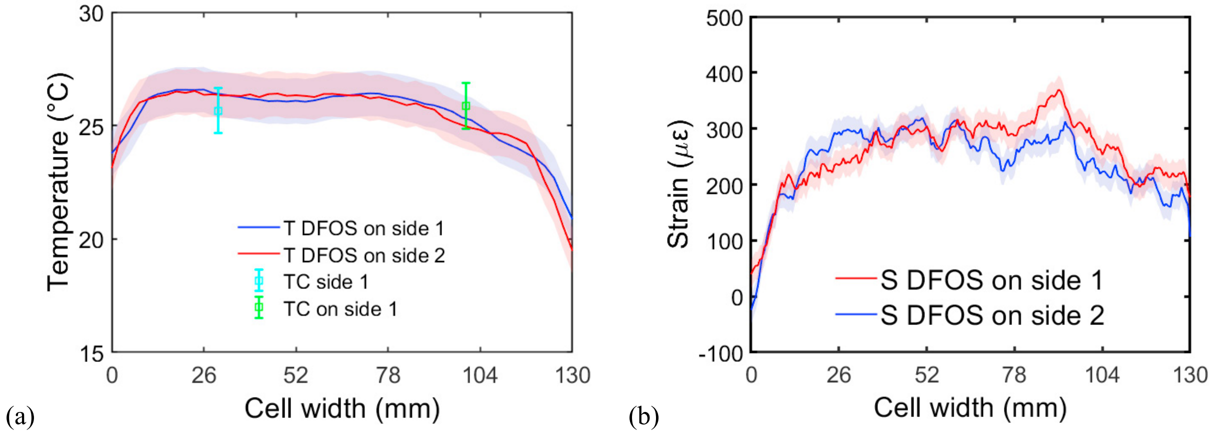

Fig. 3. Comparison between cell front and back distributed measurements. (a) Temperature results; (b) Strain results.

In Fig. 3 (a), the temperature spatial gradient in a cell region is presented. From the figure, no temperature difference can be observed between the front and the back of the cell, has the error bands of the temperature profiles registered on the front and the back of the cell always overlap.

4.2. Strain gradients

In Fig. 3 (b), a comparison between strain measured in each cell region front and back of the cell is presented at a given time instant. The distributed strain value results to be quite uniform between the front and the back.

Fig. 4 shows the evolution of one point over time. It is possible to see that during the rest period when no current is flowing, the strain value goes back to a no strain condition, and the temperature value goes back to the chamber temperature, set to 25 °C. When a current is applied, the temperature and strain increase become very evident in the 3C and 5C steps. Both temperature and strain present a very similar evolution over time.

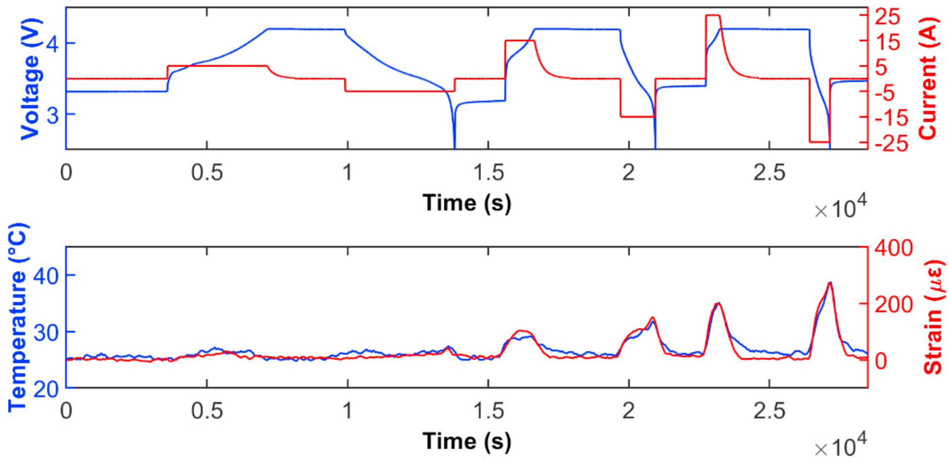

Fig. 4. Temperature and strain evolution over time when cycling at 25 °C.

5. Conclusion

To know the temperature distribution in a cell and between cells is fundamental to guarantee a good state of health of the battery and safety. It has been demonstrated that Rayleigh scattering DFOS are suitable to monitor both temperature and strain gradients on Li-ion cells surface during cycling. In the test performed, no evident temperature and strain spatial gradients have been registered. This behaviour is in line with the fact that the cells under test are fresh cells. However, because the test setup has been able to provide reliable and stable results, these cells will be further cycled in order to produce an ageing effect and the temperature and strain gradients will be monitored in order to highlight possible uneven distributions and abnormal changes. Future work will also include the use of DFOS to perform internal in-situ and in-operando monitoring with DFOS.

References

Bao, X., Chen, L., 2012. Recent progress in distributed fiber optic sensors. Sensor 12 (7), 8601–8639.

Chen, S. C., Wan, C. C., Wang, Y. Y., 2005. Thermal analysis of lithium-ion batteries. Journal of Power Sources 140, 111–124.

Ganguli, A., Saha, B., Raghavan, A., Kiesel, P., Arakaki, K., Schuh, A., Schwartz, J., Hegyi, A., Sommer, L. W., Lochbaum, A., Sahu, S., Alamgir, M., 2017. Embedded fiber-optic sensing for accurate internal monitoring of cell state in advanced battery management systems part 2: Internal cell signals and utility for state estimation. Journal of Power Sources 341, 474–482.

Goutam, S., Timmermans, J., Omar, N., Van Den Bossche, P., Van Mierlo, J., 2015. Comparative Study of Surface Temperature Behavior of Commercial Li-Ion Pouch Cells of Different Chemistries and Capacities by Infrared Thermography. Energies 8, 8175–8192.

Jaiswal, A., 2017. Lithium-ion battery based renewable energy solution for off-grid electricity: A techno-economic analysis. Renewable Sustainable Energy Reviews 72, 922–934.

Kim, J., Oh, J., Lee, H., 2019. Review on battery thermal management system for electric vehicles. Applied Thermal Engineering 149, 192–212.

Lee, C., Lee, S., Chen, Y., Chung, M., Han, K., 2013. In-situ Monitoring of Temperature and Voltage in Lithium-Ion Battery by Embedded Flexible Micro Temperature and Voltage Sensor. International Journal of Electrochemical Science 8, 2968–2976.

Liao, Z., Zhang, S., Li, K., Zhang, G., Habetler, T. G., 2019. A survey of methods for monitoring and detecting thermal runaway of lithium-ion batteries. Journal of Power Sources 436, 226879.

Mukhopadhyay, A., Sheldon, B., W., 2014. Deformation and stress in electrode materials for Li-ion batteries. Progress in Materials Science 63, 58-116.

Nascimento, M., Novais, S., Ding, M. S., Ferreira, M. S., Koch, S., Passerini, S., Pinto, J. L., 2019. Internal strain and temperature discrimination with optical fiber hybrid sensors in Li-ion batteries. Journal of Power Sources 410-411, 1–9.

Raghavan, A., Kiesel, P., Sommer, L. W., Schwartz, J., Lochbaum, A., Hegyi, A., Schuh, A., Arakaki, K., Saha, B., Ganguli, A., Kim, K. H., Kim, C., Han, H. J., Kim, S., Hwang, G.-O., Chung, G.-C., Choi, B., Alamgir, M., 2017. Embedded fiber-optic sensing for accurate internal monitoring of cell state in advanced battery management systems part 1: Cell embedding method and performance. Journal of Power Sources 341, 466–473.

Raijmakers, L. H. J., Danilov, D. L., Eichel, R.-A., Notten, P. H. L., 2019. A review on various temperature-indication methods for Li-ion batteries. Applied Energy 240, 918–945.

Smith, K., Wang, C., Y., 2006. Power and thermal characterization of a lithium-ion battery pack for hybrid-electric vehicles. Journal of Power Sources 160 (1), 662–673.

Turrentine, T., 2011. Plug-in Hybrid Electric Vehicle Research Roadmap. UC Davis Plug-In Hybrid Electr. Veh. Res. Cent.

Vertiz, G., Oyarbide, M., Macicior, H., Miguel, O., Cantero, I., Fernandez de Abboiabe, P., Ulacia, I., 2014. Thermal characterization of large size lithium-ion pouch cell based on 1d electro-thermal model. Journal of Power Sources 272, 476–484.

Waldmann, T., Bisle, G., Hogg, B.-I., Stumpp, S., Danzer, M., A., Kasper, M., Axmann, P., Wohlfahrt-Mehrens, M., 2016. Influence of Cell Design on Temperatures and Temperature Gradients in Lithium-Ion Cells: An In Operando Study. Journal of The Electrochemical Society 162 (6), A921–A927.

Yi, J., Seong, U., Burm, C., Han, T., Park, S., 2013. Modeling the temperature dependence of the discharge behavior of a lithium-ion battery in low environmental temperature. Journal of Power Sources 244, 143–148.